PHYSICAL REVIEW B **96**, 081112(R) (2017)

Theoretical study of the pressure-induced topological phase transition in LaSb

Peng-Jie Guo, Huan-Cheng Yang, Kai Liu,* and Zhong-Yi Lu†
Department of Physics and Beijing Key Laboratory of Opto-electronic Functional Materials & Micro-nano Devices, Renmin University of China, Beijing 100872, China
(Received 14 June 2017; published 21 August 2017)

By using first-principles electronic structure calculations, we find that material LaSb with extreme magnetoresistance (XMR) undergoes a topological phase transition without breaking any symmetry under a hydrostatic pressure applied between 3 and 4 GPa; meanwhile, the electron-hole compensation remains in its electronic band structure. This makes LaSb an ideal platform for studying what role the topological property plays in the XMR phenomenon, in addition to the electron-hole compensation.

DOI: 10.1103/PhysRevB.96.081112

Introduction. The topological properties of realistic materials have received strong interest both theoretically and experimentally in recent years [1,2]. With protection by time-reversal symmetry, insulators can be classified into conventional band insulators and topological insulators [1,2]. Compared with conventional band insulators, topological insulators have robust conducting surface states against local perturbations [1,2]. Conceptually, a natural generalization from insulator to metal divides semimetals into trivial and nontrivial semimetals topologically in electronic structure, with the latter including Weyl, Dirac, and node-line semimetals [3]. On the other hand, different topologies are closely related [3]. For instance, a Dirac semimetal may be transformed into a Weyl semimetal by breaking time-reversal or space-inversion symmetry [3]. More interestingly, the phase transition between a topological insulator and a conventional band insulator does not break any symmetry, which surpasses Landau's phase transition theory [4,5]. This is an important breakthrough in physics theory.

For topological insulators, the gapless surface states possess many novel properties: their unique spin textures forbid the electron's backscattering under zero magnetic field [1]. For Weyl and Dirac semimetals [6–17], their fermions result in high carrier mobility as well as linear magnetoresistance [18–21]; meanwhile, their chiral anomalies render negative magnetoresistance [22–25]. Recently, the extreme magnetoresistance (XMR) as a quadratic function of magnetic field has been discovered in topologically trivial material LaSb [26,27] as well as its isostructural topologically nontrivial counterpart LaBi [28]. Previously, both the electron-hole compensation [29] and the backscattering-forbidden topological protection mechanisms [30] had been proposed to explain the XMR effect, but a consensus has not yet been achieved [31]. Through comparative studies on LaSb and LaBi, it has been realized that the electron-hole compensation plays an important role in the XMR [27,32], but what role the topological property plays is still unclear [33]. Searching for a material which shows the XMR effect with a topological phase transition under certain experimental conditions is thus very important for understanding the relationship of the XMR effect and the topological property.

Except for the topological property, LaSb and LaBi are very similar in both crystal structure and electronic band dispersion [32]. These similarities lead us to consider that LaSb may possess the same topological property as LaBi by changing lattice constants or via chemical doping. Nevertheless, chemical doping may ruin the compensation between electron-type and hole-type carriers, which is disadvantageous to studying the relationship of the XMR effect and the topological property. Instead, external pressure is a clean and powerful approach to tuning electronic structures and studying novel physical properties [34,35].

In this Rapid Communication, we have studied the evolution of the electronic structure of the XMR material LaSb with hydrostatic pressure by using first-principles electronic structure calculations. We find that LaSb undergoes a topological phase transition without breaking any symmetry under a pressure between 3 and 4 GPa. Our calculations indicate that the band inversions at the X points in the Brillouin zone result in the nontrivial topological properties of LaSb under pressure.

Method. To study the evolution of the electronic structure of LaSb with pressure, we carried out first-principles electronic structure calculations with the projector augmented wave method [36,37] as implemented in the VASP package [38–40]. For the exchange-correlation functional, we adopted two different levels in Jacob's ladder [41]: the generalized gradient approximation (GGA) and the hyper-GGA, in which the Perdew-Burke-Ernzerhof (PBE) type of formulas [42] and the screened hybrid functional [43] introduced by Heyd, Scuseria, and Ernzerhof (HSE) with the HSE06 version [44] were used, respectively. The kinetic-energy cutoff of the plane-wave basis was set to be 300 eV. For the Brillouin-zone (BZ) sampling, an $8 \times 8 \times 8$ k-point mesh was adopted for the primitive cell of the rocksalt structural crystal, which contains one formula unit. The Fermi level was broadened by a Gaussian smearing method with a width of 0.05 eV. Both cell parameters and internal atomic positions were fully relaxed. The system under hydrostatic pressures in a range of 0–14 GPa was simulated by minimizing the enthalpy of the system, namely, performing variable cell relaxation at different setting pressures [45]. When the trace of stress tensor converged to a targeting pressure, the structure relaxation stopped. The atoms were allowed to relax until all forces were smaller than 0.01 eV/Å. After the equilibrium crystal structures at different pressures were obtained, the electronic structures were studied by including the spin-orbit-coupling

*kliu@ruc.edu.cn
†zlu@ruc.edu.cn

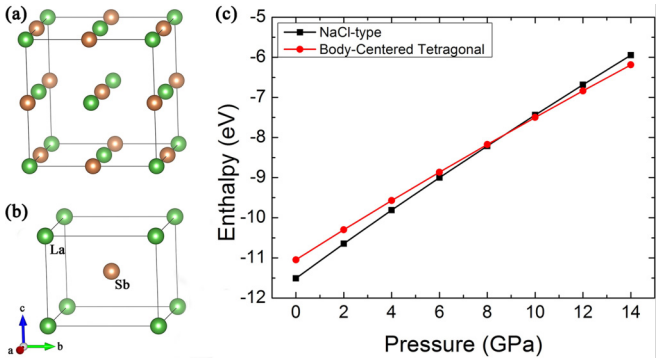

FIG. 1. (a) The NaCl-type and (b) the body-centered tetragonal crystal structures of LaSb. (c) Enthalpies of LaSb in these two forms of structures as a function of pressure.

(SOC) effect. The topological invariants were calculated using the parities of all filled states at eight time-reversal-invariant points in the BZ [46].

Results and analysis. To study the evolution of the electronic structure of LaSb with pressure, we first need to clarify its crystal structures under different pressures. Previous experiments found that LaSb undergoes a structural phase transition from a NaCl-type lattice [Fig. 1(a)] to a body-centered tetragonal lattice [Fig. 1(b)] around 11 GPa [47]. We have thus calculated the pressure-dependent enthalpies of LaSb in these two forms of crystal structures [Fig. 1(c)]. Under pressure, it is the structure with a lower enthalpy $H = E + PV$, where E is the total energy, P is the pressure, and V is the volume of the unit cell, that becomes more stable. At ambient pressure, the enthalpy of the rocksalt structure is lower than that of the body-centered tetragonal structure, showing that the former is more stable. With increasing pressure, the enthalpies of both structures rise up gradually. However, the enthalpy of the rocksalt structure grows faster than that of the body-centered tetragonal structure, and around 9 GPa there exists a crossover. This result verifies that LaSb undergoes a pressure-induced structural phase transition at ∼9 GPa, which is in accord with previous measurements [47].

Once the crystal structure is determined, the band structure of LaSb can be studied under pressure. We first focus on the rocksalt structure at ambient pressure. It is well known that a La atom possesses three valence electrons, while an Sb atom possesses five valence electrons. If an Sb atom can completely obtain three valence electrons from a La atom in LaSb, it should be an insulator. We have investigated the band structure of LaSb along high-symmetry directions in the BZ by using the PBE and HSE06 functionals and including the SOC effect (Fig. 2). Here, only the bands around the Fermi level are presented. We find that there is a small overlap between the valence and conduction bands of LaSb, demonstrating that LaSb is a semimetal, which is in agreement with the observation in the previous transport experiment [26]. On the other hand, there is a band inversion around the high-symmetry point X in the BZ for the band structure calculated with the PBE functional at GGA level [Fig. 2(a)], but no band inversion with the HSE06 functional at hyper-GGA level [Fig. 2(b)]. In addition, our previous calculations

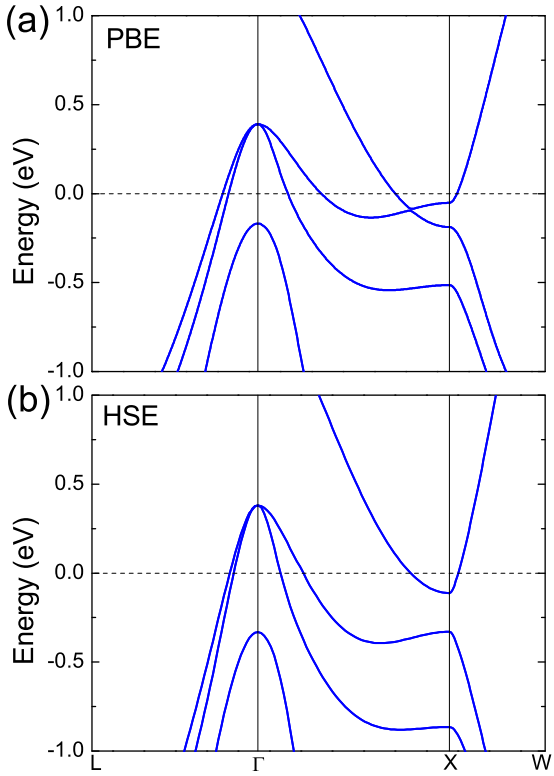

FIG. 2. Band structures of LaSb in NaCl-type structure along high-symmetry directions of the Brillouin zone calculated with the (a) PBE and (b) HSE06 functionals including the SOC effect at ambient pressure. The Fermi level is set to zero.

with the modified Becke-Johnson exchange potential [48,49] at meta-GGA level also indicate no band inversion around the X points [32]. Since the band inversion is a very important feature for nontrivial topological electronic structure, LaSb shows different topologies in electronic structure in calculations at different exchange-correlation functional levels. From the experimental side, the angle-resolved photoemission spectroscopy (ARPES) measurement clearly demonstrates that there is no band inversion around the X points, showing that LaSb is a topologically trivial semimetal at ambient pressure [27]. This illustrates that the calculated band structures at higher (meta-GGA and hyper-GGA) levels agree better with the one obtained in the ARPES experiment.

We know that different from chemical doping, pressure can effectively tune the electronic structures of materials without introducing foreign atomic species. So one may wonder whether the nontrivial topology would take place in the electronic structure of LaSb with increasing pressure, especially before the structural phase transition. In order to answer this question, we have calculated the band structures of LaSb under pressures from 1 to 8 GPa, in which the rocksalt crystal structure and the HSE functional were used, as suggested by the above results (Figs. 1 and 2). We find that from 1 to 3 GPa there is no band inversion around the X points, but from 4 to 8 GPa the band inversion takes place. For simplicity, we just display the representative band structure at 3 GPa before the transition [Fig. 3(a)] and the one at 4 GPa after the transition [Fig. 3(b)].

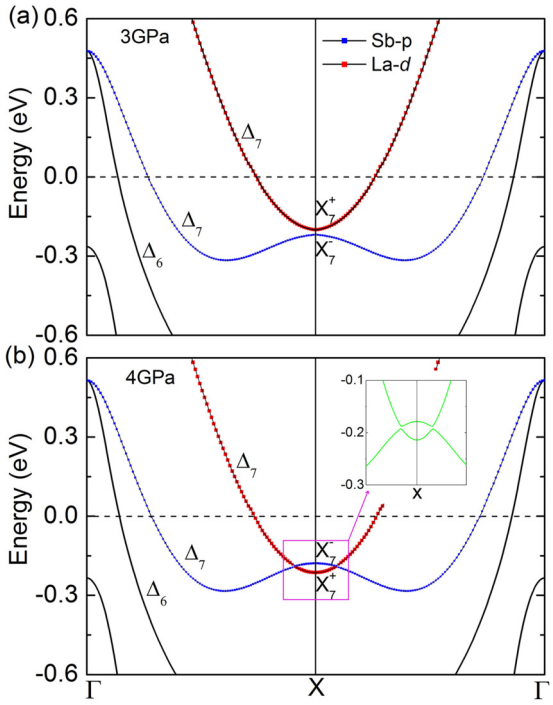

FIG. 3. Orbital characteristics and symmetries of the two bands around the X points near the Fermi level for LaSb in NaCl-type structure calculated with the HSE06 functional and including the SOC effect at (a) 3 GPa and (b) 4 GPa. The Fermi level is set to zero. The signs $\pm$ indicate the parities of corresponding states, respectively. The inset shows the enlarged region around the band crossing.

More information is needed to get in-depth insight into the two (crossing) bands around the X points, as shown in Fig. 3. The symmetry for the $\Gamma-X$ direction in the BZ of LaSb in rocksalt structure is C_{4v} double group when the SOC effect is included. Considering the fact that LaSb has both time-reversal and space-inversion symmetries, the band crossing around the X points may make LaSb a Dirac semimetal. Accordingly, we analyze the related orbital weights, symmetries, and wave-function parities of these two crossing bands. With orbital weight analysis of the bands near the Fermi level along the $\Gamma-X$ direction, the valence (lower) band consists mainly of Sb p orbitals, while the conduction (upper) band is primarily contributed by La d (t_{2g}) orbitals. Before the band crossing, for example, at 3 GPa [Fig. 3(a)], the symmetries of the valence band are Δ_7 along the $\Gamma-X$ direction and X_7^- (odd parity) at the X points, respectively, while those of the conduction band are Δ_7 along the $\Gamma-X$ direction and X_7^+ (even parity) at the X points, respectively. Since the symmetries of the valence and conduction bands both belong to the same irreducible representation Δ_7 of the C_{4v} double group along the $\Gamma-X$ direction, their crossing, for example, at 4 GPa [Fig. 3(b)], opens a gap when the SOC effect is included (see the inset). This indicates that LaSb is not a Dirac semimetal. Nevertheless, as there are inversed bands with opposite parities around three equivalent X points in the BZ at 4 GPa [Fig. 3(b)], LaSb may be a topological insulator defined on a curved Fermi surface.

In order to verify the topological property of LaSb under pressure, we have further calculated its Z_2 topological invariants. Different from the two-dimensional quantum spin Hall effect, the three-dimensional topological insulator has four Z_2 topological invariants [50]. If a material has both time-reversal and space-inversion symmetries, its Z_2 topological invariants can be calculated from the parities of filled states at all time-reversal-invariant points. The value (1 or 0) of the first Z_2 topological invariant, ν_0, indicates whether a topological insulator is strong or weak. Here, we have calculated this important index ν_0 as a function of pressure as displayed in Fig. 4. As we see around the X points, there is no band inversion at 3 GPa and the ν_0 is 0, while at 4 GPa the band inversion takes place and the ν_0 changes to 1. All detailed parities of the filled states at eight time-reversal-invariant points before and after the jump of ν_0 are listed in Tables I and II, respectively. By comparing the parities of all these filled states, we find that the inversion of the two bands around the X points nearest to the Fermi level, as shown in Fig. 3, leads to the emergence of topological phase transition. These results demonstrate that there is a topological phase transition before the structural transition in NaCl-type LaSb with increasing pressure.

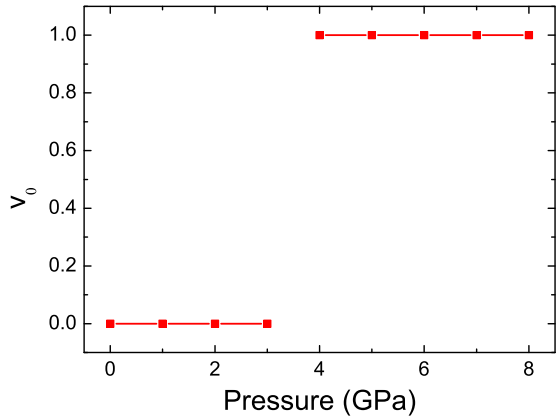

FIG. 4. The topological invariants ν_0 of LaSb in NaCl-type structure as a function of pressure.

Discussion. Previous studies showed that LaSb and LaBi possess different topological properties at ambient pressure [27,32,51,52]. Given that LaSb and LaBi own the same crystal structures and valence electron configurations, one may straightforwardly think that they should give out similar band structures. Nevertheless, the distinct difference between the band structures of LaSb and LaBi is that LaBi takes band

TABLE I. The parities of all filled states of LaSb in NaCl-type structure at eight time-reversal-invariant points in the Brillouin zone before the topological phase transition.

No.	Γ	L	L	L	L	X	X	X	Total
1	−	−	−	−	−	−	−	−	+
3	−	−	−	−	−	−	−	−	+
5	−	−	−	−	−	−	−	−	+
7	+	−	−	−	−	+	+	+	+
9	−	+	+	+	+	−	−	−	+
11	−	+	+	+	+	−	−	−	+
13	−	+	+	+	+	−	−	−	+
Total	+	+	+	+	+	+	+	+	(+)

TABLE II. The parities of all filled states of LaSb in NaCl-type structure at eight time-reversal-invariant points in the Brillouin zone after the topological phase transition.

No.	Γ	*L*	*L*	*L*	*L*	*X*	*X*	*X*	Total
1	−	−	−	−	−	−	−	−	+
3	−	−	−	−	−	−	−	−	+
5	−	−	−	−	−	−	−	−	+
7	+	−	−	−	−	+	+	+	+
9	−	+	+	+	+	−	−	−	+
11	−	+	+	+	+	−	−	−	+
13	−	+	+	+	+	+	+	+	−
Total	+	+	+	+	+	−	−	−	(−)

inversions at the time-reversal-invariant *X* points, which makes it topologically nontrivial, while LaSb does not have any band inversion. Compared with the Sb atom, the Bi atom has a stronger SOC effect and its $6p$ orbital electrons are more extended. On the other hand, the pressure is an effective approach to tune the electronic properties of materials, and the valence electrons generally become more extended due to the band broadening under pressure. Thus LaSb may also have band inversions at the *X* points under certain pressure. From the above calculations (Fig. 4), LaSb does undergo a topological phase transition with the increase of pressure. Very recently, the nontrivial Berry phase has been observed by both Shubnikov–de Haas and de Haas–van Alphen oscillation experiments for LaBi [53]. This is also to say, the topological phase transition of LaSb under pressure may be verified by observing the nontrivial Berry phase in experiment.

Another important property of LaSb is its extreme magnetoresistance [26]. In semimetal LaSb, there exists a small overlap between the valence and conduction bands [Fig. 2(b)]. Supposing that an Sb atom can completely obtain three valence electrons of a La atom, LaSb would become an insulator. Thus if all electrons in the conduction band of LaSb are transferred to the valence band, the latter would be fully filled. In this sense, it is easy to understand that the electronlike and holelike carrier concentrations are equal in LaSb, as evidenced by our previous calculations [32] and related experiments [27]. Meanwhile, transport experiments have discovered that the carrier mobilities are very high in LaSb [26]. Accordingly, within the semiclassical band model, the electron-hole compensation and high carrier mobilities together can naturally explain the XMR effect [28,29,32].

In addition to the electron-hole compensation, the topological protection has also been proposed to explain the XMR effect. Since many XMR materials are topologically nontrivial [20,21,25,29,54], it is very important to explore the relationship of the XMR effect and the topological property. For LaSb, with increasing pressure, our calculations indicate that the small overlap between the valence and conduction bands still exists (Fig. 3), thus the charge compensation also holds. Considering that the charge compensation accompanies the topological phase transition in LaSb under pressure, as shown by the calculations, if the MR of LaSb shows sharp even discontinuous variation around the transition pressure in magnetic transport experiments, the topological property will have a substantial impact on the XMR, otherwise it will have no dominating effect on the XMR. In this sense, the NaCl-type LaSb under pressure is a promising platform to clarify this relationship.

Summary. By using first-principles electronic structure calculations, we find that the XMR material LaSb undergoes a topological phase transition without breaking any symmetry under hydrostatic pressure. Irrespective of topological phase transition, the electron-type and hole-type carriers remain compensated. Considering that both a charge-compensation mechanism and a topological protection mechanism have been proposed to explain the XMR effect, the pressed LaSb provides an ideal playground for studying the role that the topological property plays in the XMR phenomenon.

Acknowledgments. We thank Yuan-Yao He, Tao Li, He-Chang Lei, and Shan-Cai Wang for helpful conversations. This work was supported by National Key R&D Program of China (Grant No. 2017YFA0302903), National Natural Science Foundation of China (Grants No. 11474356 and No. 91421304), the Fundamental Research Funds for the Central Universities, and the Research Funds of Renmin University of China (Grants No. 14XNLQ03 and No. 16XNLQ01). Computational resources were provided by the Physical Laboratory of High Performance Computing at Renmin University of China.

[1] M. Z. Hasan and C. L. Kane, Rev. Mod. Phys. **82**, 3045 (2010).
[2] X.-L. Qi and S.-C. Zhang, Rev. Mod. Phys. **83**, 1057 (2011).
[3] H.-M. Weng, X. Dai, and Z. Fang, J. Phys.: Condens. Matter **28**, 303001 (2016).
[4] D. J. Thouless, M. Kohmoto, M. P. Nightingale, and M. D. Nijs, Phys. Rev. Lett. **49**, 405 (1982).
[5] X.-G. Wen, Adv. Phys. **44**, 405 (1995).
[6] X.-G. Wan, A. M. Turner, A. Vishwanath, and S. Y. Savrasov, Phys. Rev. B **83**, 205101 (2011).
[7] Z.-J. Wang, Y. Sun, X.-Q. Chen, C. Franchini, G. Xu, H.-M. Weng, X. Dai, and Z. Fang, Phys. Rev. B **85**, 195320 (2012).
[8] Z.-K. Liu, B. Zhou, Y. Zhang, Z.-J. Wang, H.-M. Weng, D. Prabhakaran, S-K. Mo, Z.-X. Shen, Z. Fang, X. Dai *et al.*, Science **343**, 864 (2014).
[9] Z.-J. Wang, H.-M. Weng, Q. Wu, X. Dai, and Z. Fang, Phys. Rev. B **88**, 125427 (2013).
[10] Z.-K. Liu, J. Jiang, B. Zhou, Z. J. Wang, Y. Zhang, H. M. Weng, D. Prabhakaran, S.-K. Mo, H. Peng, P. Dudin *et al.*, Nat. Mater. **13**, 677 (2014).
[11] H.-M. Weng, C. Fang, Z. Fang, B. A. Bernevig, and X. Dai, Phys. Rev. X **5**, 011029 (2015).
[12] B. Q. Lv, H. M. Weng, B. B. Fu, X. P. Wang, H. Miao, J. Ma, P. Richard, X. C. Huang, L. X. Zhao, G. F. Chen *et al.*, Phys. Rev. X **5**, 031013 (2015).

[13] S.-Y. Xu, I. Belopolski, N. Alidoust, M. Neupane, G. Bian, C.-L. Zhang, R. Sankar, G.-Q. Chang, Z.-J. Yuan, C.-C. Lee *et al.*, Science **349**, 613 (2015).
[14] B. Q. Lv, N. Xu, H. M. Weng, J. Z. Ma, P. Richard, X. C. Huang, L. X. Zhao, G. F. Chen, C. E. Matt, F. Bisti *et al.*, Nat. Phys. **11**, 724 (2015).
[15] H.-M. Weng, C. Fang, Z. Fang, and X. Dai, Phys. Rev. B **93**, 241202(R) (2016).
[16] Z. Zhu, G. W. Winkler, Q. S. Wu, J. Li, and A. A. Soluyanov, Phys. Rev. X **6**, 031003 (2016).
[17] B. Q. Lv, Z.-L. Feng, Q.-N. Xu, X. Gao, J.-Z. Ma, L.-Y. Kong, P. Richard, Y.-B. Huang, V. N. Strocov, C. Fang, H.-M. Weng, Y.-G. Shi, T. Qian, and H. Ding, Nature (London) **546**, 627 (2017).
[18] A. A. Abrikosov, Phys. Rev. B **58**, 2788 (1998).
[19] M. Neupane, S.-Y. Xu, R. Sankar, N. Alidoust, G. Bian, C. Liu, I. Belopolski, T.-R. Chang, H.-T. Jeng, H. Lin *et al.*, Nat. Commun. **5**, 3786 (2014).
[20] T. Liang, Q. Gibson, M. N. Ali, M. Liu, R. J. Cava, and N. P. Ong, Nat. Mater. **14**, 280 (2015).
[21] C. Shekhar, A. K. Nayak, Y. Sun, M. Schmidt, M. Nicklas, I. Leermakers, U. Zeitler, Z.-K. Liu, Y.-L. Chen, W. Schnelle *et al.*, Nat. Phys. **11**, 645 (2015).
[22] H. B. Nielsen and M. Ninomiya, Phys. Lett. B **130**, 389 (1983).
[23] S. A. Parameswaran, T. Grover, D. A. Abanin, D. A. Pesin, and A. Vishwanath, Phys. Rev. X **4**, 031035 (2014).
[24] J. Xiong, S. K. Kushwaha, T. Liang, J. W. Krizan, M. Hirschberger, W.-D. Wang, R. J. Cava, and N. P. Ong, Science **350**, 413 (2015).
[25] X.-C. Huang, L.-X. Zhao, Y.-J. Long, P.-P. Wang, D. Chen, Z.-H. Yang, H. Liang, M.-Q. Xue, H.-M. Weng, Z. Fang *et al.*, Phys. Rev. X **5**, 031023 (2015).
[26] F. F. Tafti, Q. D. Gibson, S. K. Kushwaha, N. Haldolaarachchige, and R. J. Cava, Nat. Phys. **12**, 272 (2016).
[27] L.-K. Zeng, R. Lou, D.-S. Wu, Q. N. Xu, P.-J. Guo, L.-Y. Kong, Y.-G. Zhong, J.-Z. Ma, B.-B. Fu, P. Richard *et al.*, Phys. Rev. Lett. **117**, 127204 (2016).
[28] S.-S. Sun, Q. Wang, P.-J. Guo, K. Liu, and H.-C. Lei, New J. Phys. **18**, 082002 (2016).
[29] M. N. Ali, J. Xiong, S. Flynn, J. Tao, Q. D. Gibson, L. M. Schoop, T. Liang, N. Haldolaarachchige, M. Hirschberger, N. P. Ong, and R. J. Cava, Nature (London) **514**, 205 (2014).
[30] J. Jiang, F. Tang, X.-C. Pan, H.-M. Liu, X.-H. Niu, Y.-X. Wang, D.-F. Xu, H.-F. Yang, B.-P. Xie, F.-Q. Song *et al.*, Phys. Rev. Lett. **115**, 166601 (2015).
[31] J.-F. He, C.-F. Zhang, N. J. Ghimire, T. Liang, C.-J. Jia, J. Jiang, S-J. Tang, S.-D. Chen, Y. He, S.-K. Mo *et al.*, Phys. Rev. Lett. **117**, 267201 (2016).
[32] P.-J. Guo, H.-C. Yang, B.-J. Zhang, K. Liu, and Z.-Y. Lu, Phys. Rev. B **93**, 235142 (2016).
[33] X.-H. Niu, D.-F. Xu, Y.-H. Bai, Q. Song, X.-P. Shen, B.-P. Xie, Z. Sun, Y.-B. Huang, D. C. Peets, and D.-L. Feng, Phys. Rev. B **94**, 165163 (2016).
[34] L. Gao, Y.-Y. Xue, F. Chen, Q. Xiong, R.-L. Meng, D. Ramirez, C.-W. Chu, J. H. Eggert, and H.-K. Mao, Phys. Rev. B **50**, 4260(R) (1994).
[35] Z.-H. Chi, X.-M. Zhao, H.-D. Zhang, A. F. Goncharov, S. S. Lobanov, T. Kagayama, M. Sakata, and X.-J. Chen, Phys. Rev. Lett. **113**, 036802 (2014).
[36] P. E. Blöchl, Phys. Rev. B **50**, 17953 (1994).
[37] G. Kresse and D. Joubert, Phys. Rev. B **59**, 1758 (1999).
[38] G. Kresse and J. Hafner, Phys. Rev. B **47**, 558 (1993).
[39] G. Kresse and J. Furthmüller, Comput. Mater. Sci. **6**, 15 (1996).
[40] G. Kresse and J. Furthmüller, Phys. Rev. B **54**, 11169 (1996).
[41] J. P. Perdew, A. Ruzsinszky, J.-M. Tao, V. N. Staroverov, G. E. Scuseria, and G. I. Csonka, J. Chem. Phys. **123**, 062201 (2005).
[42] J. P. Perdew, K. Burke, and M. Ernzerhof, Phys. Rev. Lett. **77**, 3865 (1996).
[43] J. Heyd, G. E. Scuseria, and M. Ernzerhof, J. Chem. Phys. **118**, 8207 (2003); **124**, 219906 (2006).
[44] A. V. Krukau, O. A. Vydrov, A. F. Izmaylov, and G. E. Scuseria, J. Chem. Phys. **125**, 224106 (2006).
[45] Q.-Q. Ye, K. Liu, and Z.-Y. Lu, Phys. Rev. B **88**, 205130 (2013).
[46] L. Fu and C. L. Kane, Phys. Rev. B **76**, 045302 (2007).
[47] J. M. Leger, D. Ravot, and J. Rossat-Mignod, J. Phys. C: Solid State Phys. **17**, 4935 (1984).
[48] A. D. Becke and E. R. Johnson, J. Chem. Phys. **124**, 221101 (2006).
[49] F. Tran and P. Blaha, Phys. Rev. Lett. **102**, 226401 (2009).
[50] L. Fu, C. L. Kane, and E. J. Mele, Phys. Rev. Lett. **98**, 106803 (2007).
[51] J. Nayak, S.-C. Wu, N. Kumar, C. Shekhar, S. Singh, J. Fink, E. E. D. Rienks, G. H. Fecher, S. S. P. Parkin, B. Yan, and C. Felser, Nat. Commun. **8**, 13942 (2017).
[52] R. Lou, B.-B. Fu, Q. N. Xu, P.-J. Guo, L.-Y. Kong, L.-K. Zeng, J.-Z. Ma, P. Richard, C. Fang, Y.-B. Huang *et al.*, Phys. Rev. B **95**, 115140 (2017).
[53] R. Singha, B. Satpati, and P. Mandal, Sci. Rep. **7**, 6321 (2017).
[54] J. Feng, Y. Pang, D. Wu, Z. Wang, H.-M. Weng, J. Li, X. Dai, Z. Fang, Y.-G. Shi, and L. Lu, Phys. Rev. B **92**, 081306 (2015).